CrossMark

Approaches to Middle Stone Age landscape archaeology in tropical Africa

David K. Wright [a,b,*], Jessica C. Thompson [c], Flora Schilt [d], Andrew S. Cohen [e], Jeong-Heon Choi [f], Julio Mercader [g], Sheila Nightingale [h], Christopher E. Miller [i], Susan M. Mentzer [d,j], Dale Walde [g], Menno Welling [k], Elizabeth Gomani-Chindebvu [l]

[a] Department of Archaeology and Art History, Seoul National University, Seoul, 08826, South Korea
[b] University of York, Department of Archaeology, York, YO1 7EP, United Kingdom
[c] Department of Anthropology, Emory University, Atlanta, GA, 30322, USA
[d] Institute for Archaeological Sciences, University of Tübingen, Tübingen, 72070, Germany
[e] Departments of Geosciences AND Ecology and Evolutionary Biology, University of Arizona, Tucson, AZ, 85721, USA
[f] Geochronology Group, Korean Basic Science Institute, Chungbuk, 363-883, South Korea
[g] Department of Anthropology and Archaeology, University of Calgary, Calgary, AB, T2N 1N4, Canada
[h] Department of Anthropology, City University of New York, New York, NY, 10016, USA
[i] Institute for Archaeological Sciences AND Senckenberg Centre for Human Evolution and Paleoenvironment, University of Tübingen, Tübingen, 72070, Germany
[j] School of Anthropology, University of Arizona, Tucson, AZ, 85721, USA
[k] African Heritage Research and Consultancy, PO Box 622, Zomba, Malawi
[l] Malawi Ministry of Tourism, Wildlife, and Culture, Lilongwe 3, Malawi

ARTICLE INFO

ABSTRACT

The Southern Montane Forest-Grassland mosaic ecosystem in the humid subtropics southern Rift Valley of Africa comprised the environmental context for a large area in which modern human evolution and dispersal occurred. Variable climatic conditions during the Late Pleistocene have ranged between humid and hyperarid, changing the character of the ecosystem and transforming it at different points in time into a barrier, a refuge, and a corridor between southern and eastern African populations. Alluvial fans presently blanket the areas adjacent to major river systems, which were key areas of prehistoric human habitation. These sets of variables have created conditions that are both challenging and advantageous to conduct archaeological research. Lateritic soil development has resulted in poor organic preservation and facilitated insect bioturbation, which has demanded an integrated micro-macro scale approach to building a reliable geochronology. An integrated field and analytical methodology has also been employed to identify the nature and degree of post-depositional movement in alluvial deposits, which preserve a wide range of spatial integrity levels in buried stone artifact assemblages between 47 and 30 ka in Karonga, northern Malawi. This paper describes the methodological advances taken toward understanding open-air Middle Stone Age archaeology in sub-tropical Africa, and explores the inferential potential for understanding Pleistocene human ecology in the important southern Rift Valley region.

1. Introduction

The Middle Stone Age (MSA) of Africa shows some of the earliest clear archaeological evidence for many behaviors that are either unique to or especially well developed in modern humans (d'Errico and Stringer, 2011; McBrearty and Brooks, 2000). As a typo-technological unit, the MSA is defined by the significant presence of prepared core technology, nascent forms of symbolic expression and the absence of large bifacial tools such as handaxes, spanning

* Corresponding author. Department of Archaeology and Art History, Seoul National University, Seoul, 08826, South Korea.
E-mail addresses: msafiri@snu.ac.kr (D.K. Wright), jessica.thompson@emory.edu (J.C. Thompson), fcschilt@gmail.com (F. Schilt), cohen@email.arizona.edu (A.S. Cohen), jhchoi@kbsi.re.kr (J.-H. Choi), mercader@ucalgary.ca (J. Mercader), snightingale@gradcenter.cuny.edu (S. Nightingale), christopher.miller@uni-tuebingen.de (C.E. Miller), susan.mentzer@ifu.uni-tuebingen.de (S.M. Mentzer), walde@ucalgary.ca (D. Walde), welling@africanheritage.mw (M. Welling), egomanichindebvu@yahoo.com (E. Gomani-Chindebvu).

from ca. 285 thousand years ago (ka) to ca. 20 ka (Conard, 2015; Sahle et al., 2014; Tryon and Faith, 2013). Much of the evidence for the MSA comes from more temperate parts of Africa, both in the southern (Brown et al., 2012; Henshilwood et al., 2011; Lombard, 2011; Porraz et al., 2013) and northern parts of the continent (d'Errico et al., 2009; Linstädter et al., 2012). This record is also heavily biased toward the long archives of human behavior that are found in cave or rock shelter sites.

There is a need to advance methods to understand the depositional and taphonomic context for open-air MSA sites in tropical and subtropical ecosystems. New geoarchaeological approaches are tailored for these situations and have equipped researchers with tools to investigate the environmental backdrop of cultural diversifications by MSA people that were critical in defining the trajectory of Pleistocene human evolution. Herein, we present a multi-tiered approach to the interpretation of open-air MSA archaeological sites in alluvial settings in Karonga, northern Malawi, which draws from well-vetted techniques but combines them in novel ways. High-resolution spatial analysis using 3-dimensional (3D) Geographical Information Systems (GIS) and refitting from piece-plotted archaeological excavations reveal whether archaeological deposits have been disturbed by secondary processes. Micromorphological data provide information about modes of deposition, pedogenesis and bioturbation, contextualizing their potential to alter the Optically Stimulated Luminescence (OSL) dosing environment used to estimate the ages of the sites. Integration of data from phytoliths allows for cross-referencing of macro- and micro-scale sedimentary environment observations, and developing terrestrial vegetation histories. Finally, by comparing data from archaeological contexts with a nearby high-resolution lacustrine paleoenvironmental record from Lake Malawi and adjacent regions, a model can be developed that explains human behavioral patterns in response to climatic changes throughout the Late Pleistocene. We describe these approaches to MSA sites in the tropics with specific reference to Chaminade II (CHA-II), which is typical of many archaeological sites in the Karonga District in its depositional context and artifactual composition.

2. Background

The southern Rift Valley of Africa is a critical, yet little-explored geographic transition zone for understanding the evolution and diversification of MSA populations across Africa. Near the modern town of Karonga, Malawi (Fig. 1), pioneering research by Desmond Clark and Vance Haynes in the 1960s (Clark and Haynes, 1970; Clark et al., 1970, 1966), followed by more intensive geoarchaeological investigations by Zefe Kaufulu (1983, 1990), demonstrated the high potential of the region's archaeological record to reveal information about the MSA in tropical and subtropical ecosystems. However, the lack of absolute ages made it difficult to tie the human behavioral record to the significant paleoenvironmental changes the area experienced over the course of the Late Pleistocene (Cohen et al., 2007; Lane et al., 2013; Scholz et al., 2011, 2007). More recently, work by the Malawi Earlier-Middle Stone Age Project (MEMSAP) has revised interpretations of sites first studied by Clark and colleagues (Clark and Haynes, 1970; Clark et al., 1970, 1966) describing the spatial-temporal distribution and attributes of artifactual assemblages and artifact raw material sources near Karonga (Thompson et al., 2014, 2012, 2013; Wright et al., 2014; Zipkin et al., 2015).

Tropical and subtropical regions of Africa are located within the most productive biotic environments in the world (Grace et al., 2006), and, as such, present a unique cluster of opportunities and pitfalls for archaeological research. In addition to intensive and

sustained agriculture and other land use practices that involve movement of sediment, bioturbation from termites (e.g., Crossley, 1986; McBrearty, 1990; Mercader et al., 2003), burrowing mammals and lizards, and fluvial winnowing (Schick, 1987; Yellen, 1996) all provide opportunity for disturbance of primary archaeological deposits. In addition, groundwater percolation (Schick, 1987; Sitzia et al., 2012; Stewart et al., 2012; Yellen, 1996), biomantle formation ("soil upbuilding"; Ahr et al., 2012; Araujo, 2013; Johnson et al., 2005; Phillips and Lorz, 2008; Van Nest, 2002) and pedogenic processes translocating minerals down the solum (Eren et al., 2014; Feathers, 2002; Gliganic et al., 2012) have been identified as potential factors affecting site taphonomy.

In northern Malawi, downwarping and fault-trough sedimentation during the Middle to Late Pleistocene (Betzler and Ring, 1995; Ebinger et al., 1993) in combination with variable climatic conditions (Crossley, 1984; Stone et al., 2011) activated alluvial fans and streams, which created riparian environments attractive to MSA people (Thompson et al., 2014, 2012; Wright et al., 2014). The remains of MSA activities in the Karonga region are embedded in remnants of an alluvial fan system known as the Chitimwe Beds (Clark and Haynes, 1970; Clark et al., 1970; Kaufulu, 1990; Wright et al., 2014). Alluvial fans can rapidly bury occupation surfaces and rework older deposits. Because many of the sediments have been subsequently modified through pedogenesis and bioturbation, artifacts can change their stratigraphic position and are often found in association with paleosols that formed at a later date. The materials and methods employed by MEMSAP were tailored to address these specific taphonomic conditions of the Karonga sites, which fall within an equatorial savanna with a dry winter (Aw) of the Köppen-Geiger classification system (Kottek et al., 2006).

3. Materials and methods

3.1. Landscape-scale geomorphology and site-scale sedimentology

The focus of the geomorphologic, sedimentologic and pedologic investigation concentrated on the identification of source-to-sink processes and areas of sustained landform stability in which human activity would have been plausibly preserved. Archaeological surveys and test pitting were conducted across an alluvial fan west of the modern-day town of Karonga, Malawi, which resulted in the identification of CHA-II (Fig. 1). Recording of sedimentary lithofacies involved description of sorting, bedding features, particle sizes, inclusions, rounding properties, hardness, plasticity and unit boundaries. Pedologic recording accounted for relative degrees of weathering by recording soil color, structure and the presence of authigenic and translocated minerals in the solum. Geomorphologic reconstruction of landform evolution was made by combining sedimentologic and pedologic analyses from numerous test units in combination with topographic maps. Sampling for OSL dating, micromorphology and phytolith analyses was performed to constrain environmental conditions within a dated context.

3.2. Excavation and artifact analysis

The CHA-II site ($9.955°$ S, $33.892°$ E) was excavated in 2011 and 2012. A large eroded surface to the west of CHA-II contained 100,000s of artifacts in a series of drainage gullies that incise the Chitimwe Beds. CHA-II was mechanically excavated as a 4×50 m trench to a depth of 2 m, and then excavated by hand within a central 2×32 m area. The mechanically excavated sediments were placed in ten piles of 40 m^3 each, sieved, and found to confirm an average artifact density of 1 per m^3. The center trench was excavated in natural stratigraphic units and 1×1 m squares to a maximum total depth of 4.6 m, producing in total more than 10,000
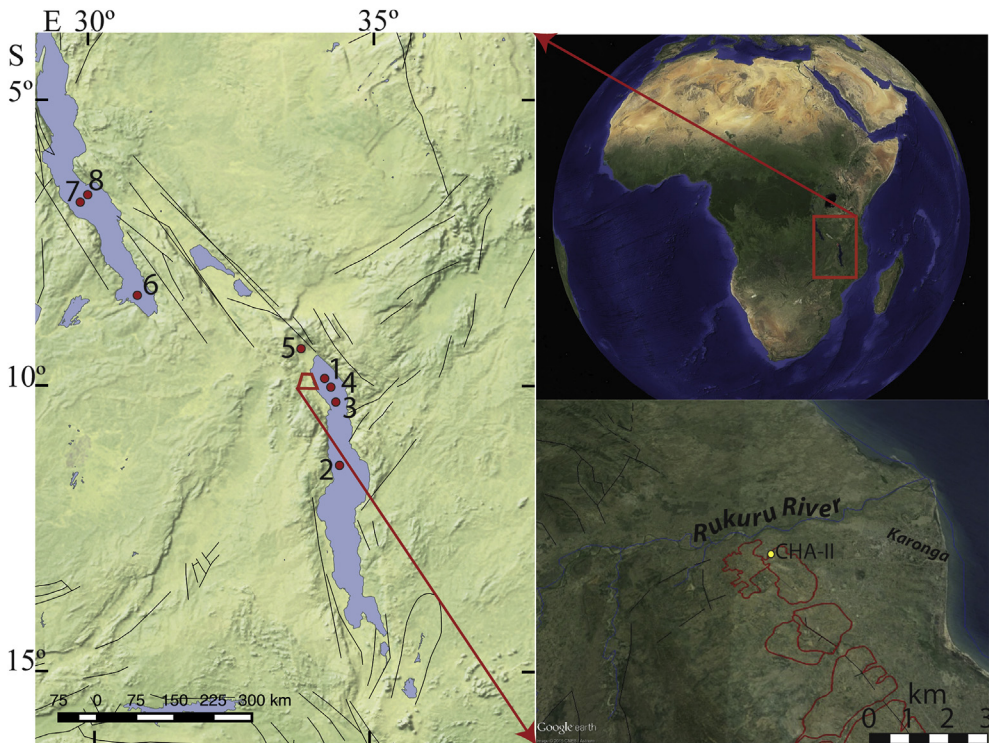
Fig. 1. Location of sites mentioned in the text. Upper right: Tropical Africa extends across the predominantly green regions. Red box denotes East-Central Africa (image from Google Earth). Left: Boxed area showing the location of paleoclimatic proxies discussed in the text. (1) Mal05—2A (Scholz et al., 2011), (2) Mal05—1C (Scholz et al., 2011), (3) M98—1P (Gasse et al., 2002; Johnson et al., 2002), (4) M98—2P (Gasse et al., 2002; Johnson et al., 2002), (5) Lake Masoko (Garcin et al., 2006; Gibert et al., 2002), (6) MPU-11 and MPU-12 (Bonnefille and Chalié, 2000; Vincens et al., 1993), (7) KH3 (Tierney et al., 2008), (8) KH4 (Tierney et al., 2008). Fault lines are black and the red polygon denotes the study area near Karonga. Lower right: Location of Chaminade-II (CHA-II) near the modern town of Karonga, fan deposits (red outlines, Chitimwe Beds) and mapped faults. (For interpretation of the references to color in this figure legend, the reader is referred to the web version of this article.)

stone artifacts. At the close of excavations, a geologic test pit was excavated at the southern end of the trench to a total depth of 6.6 m before the entire trench was backfilled. All artifacts, sedimentary units and samples were piece-plotted with a Nikon C-series 5" total station, and all artifacts with a discernable long axis were recorded with one point at each end.

Lithic artifacts were analyzed using complementary quantitative and qualitative methods on all plotted and sieved artifacts (sensu Mackay, 2008). When feasible, artifacts were also classified according to weathering stage (sensu Thompson et al., 2012), raw material, technological component (complete or fragmentary flakes and cores, flaking shatter, hammerstone, etc.), cortex cover and reduction method. Refits were sought to determine the extent of depositional reworking of the artifact assemblage, both horizontally and vertically. ArcGIS 10.2 was used to analyze the spatial relationships of artifacts of different sizes, raw materials, and rounding classes. The Optimized Hot Spot Analysis tool was used to identify clusters of artifacts within depositional units. Artifact orientation data were analyzed using Stereonet 9 to produce rose diagrams and establish if artifacts had preferred or random orientations in both the vertical and horizontal planes (McPherron, 2005).

3.3. Micromorphology

In 2012, seven block samples were collected from CHA-II for micromorphological analysis. The samples were oven-dried at 60 °C and impregnated with resin under vacuum. The resin was prepared with seven volume units of unpromoted polyester resin (Viscovoss N 55S), three volume units of styrene (styrene for synthesis) and 5—6 ml/l hardener (methyl ethyl ketone peroxide,

MEKP). After hardening, the blocks were sliced with a rock saw into slabs from which 6 × 9 cm sized thin-sections of 30-μm were produced. Micromorphological descriptions were conducted following analysis using a petrographic microscope with plane polarized light (PPL), crossed polarized light (XPL), blue light fluorescence and incident light at magnifications of 20× to 500× following Courty et al. (1989) and Stoops (2003).

A total of 90 microscopic Fourier transform infrared spectroscopic (μ-FTIR) measurements were conducted directly on the thin sections using a Cary 610 FTIR microscope attached to a Cary 660 bench (Agilent Technologies). Spectra were collected in two modes: (1) 64 co-added scans at 4 cm^{-1} resolution in transmission mode with backgrounds collected on epoxy resin over glass under typical ambient conditions and (2) 32 co-added scans at 4 cm^{-1} resolution using a germanium crystal attenuated total reflectance (Ge-ATR) objective with backgrounds on air. The transmission measurements allowed us to characterize the absorption peaks in the region of 4000—3500 cm^{-1} (Beauvais and Bertaux, 2002; Robin et al., 2013), while the Ge-ATR measurements provided peaks from 4000 to 570 cm^{-1}. Clay-sized materials were identified to kaolin and smectite group minerals by comparing the peaks to reference spectra (Downs, 2006; Salisbury and Vergo, 1991; Van de Marel and Beutelspacher, 1976) with priority given to peaks in the OH-stretching region.

3.4. OSL geochronology

Five sediment samples were collected from the profile of CHA-II for OSL dating. Quartz grains with diameters of 180—250 μm were prepared using wet sieving, acid treatments (10% HCl, 10% H_2O_2 and

40% HF) and density separation and analyzed using a TL/OSL-DA-20 Risø reader. A dose recovery test following the Single Aliquot Regeneration (SAR) protocol (Murray and Wintle, 2000, 2003) for the lowermost sample LM12-10 determined that the measured and regenerated dose ratios were within 10% for all the preheat temperatures applied (Fig. 2). Equivalent dose (D_e) values were then determined in the plateau region in which the measured D_e was independent of the preheat temperatures (Fig. 3). Dose rates (D_r) of the samples were estimated using a Canberra BEGe 5030 low-level high-resolution gamma spectrometer. OSL signals were measured based on aliquots composed of several tens of quartz grains (Small Aliquots, SA), and the final ages were derived using the Central Age Model (Galbraith and Roberts, 2012; Galbraith et al., 1999).

Two samples, LM-3161 and LM-3162, were interpreted as potentially spurious due to high over-dispersion values generated in the SA OSL analysis (Arnold and Roberts, 2009) and were therefore subjected to single-grain (SG) analysis. For SG dating, OSL signals in 1000 individual quartz grains from each sample were measured using a 10 mW Nd:YO$_4$ solid-state, diode-pumped green laser (532 nm). The optical stimulation was carried out at a readout temperature of 125 °C for 2 s, and the photon detection was through a 7-mm Hoya U-340 filter. The single grain D_e values were obtained using the SAR protocol (Murray and Wintle, 2000), and the feldspar grains were identified using IR depletion ratio (Duller, 2003). The OSL ages of the samples, together with dosimetry data and over-dispersion values, are given in Tables 1 and 2 and Fig. 4.

3.5. Local paleoenvironmental reconstruction

Phytolith samples were taken as small sediment samples from the top to the base of the southeastern profile and then continuing down the same profile on the western side of the deep geological sondage. Sixteen sediment samples were processed for the purpose of creating a vegetation landscape reconstruction. Extraction protocols were followed that were successfully employed on neighboring MSA sites (Mercader et al., 2013) and modern topsoils (Mercader et al., 2011) from the Mozambican side of the lake.

To understand the relations between specific morphotypes and taxonomic identification, the inferential baseline was grounded on the statistical analysis of local phytoliths from plants and soils (Mercader et al., 2010, 2009) and supporting references (Albert et al., 2009; Barboni and Bremond, 2009; Bremond et al., 2008; Fernández Honaine et al., 2009; Novello et al., 2012; Piperno and Pearsall, 1998; Runge, 1999; Twiss et al., 1969). Preservation was adequate for morphometric analysis and type identification, although marked dissolution was a concern in some samples. A
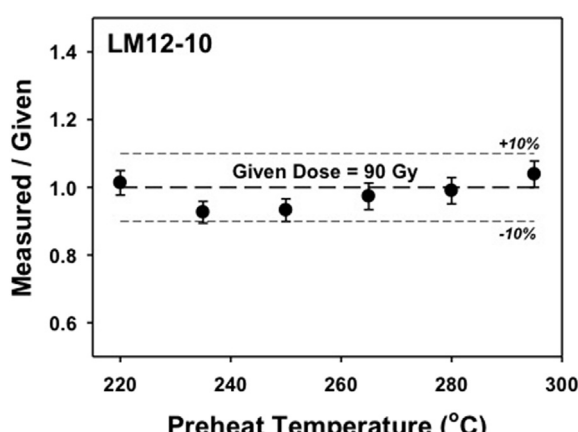
Fig. 2. Dose recovery test for LM12-10.
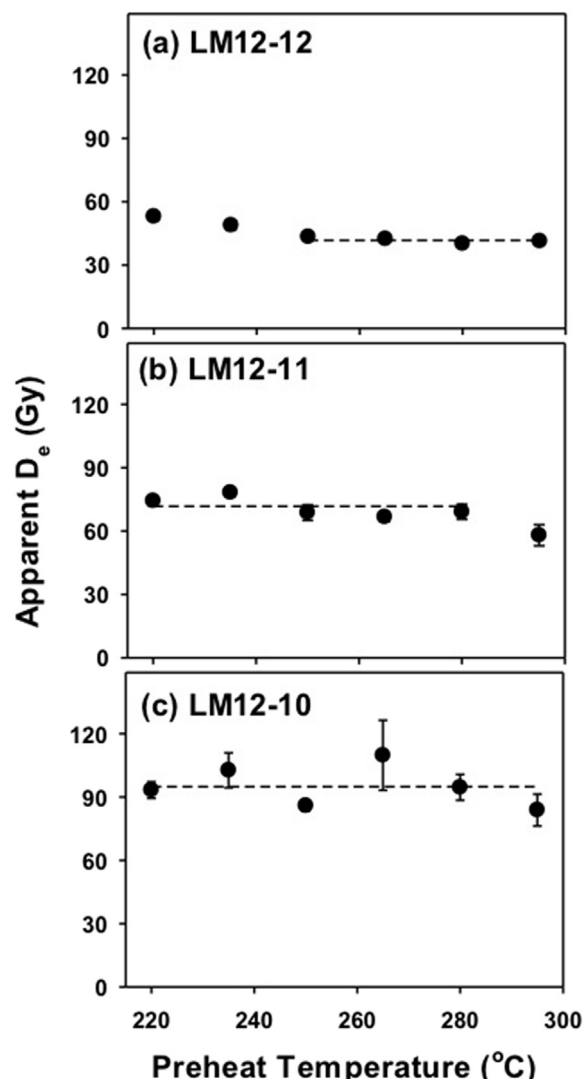
Fig. 3. Preheat plateau tests and equivalent dose (D_e) of LM12-10, LM12-11, LM12-12.

total of 6089 discrete phytolith shapes were classified and grouped into 59 morphotypes (Fig. 5).

4. The Chaminade-II sequence

4.1. Lithology and site formation processes

MSA artifacts at CHA-II were entrained in alluvial fan deposits, but sedimentation of the site changed through time, reflecting different ecological conditions commonly found in tropical Africa. Site formation processes were interpreted on the basis of micro-scale (Supplementary Online Material 1) and macro-scale analysis of sediments and pedofeatures (Fig. 6).

Units 1 and 2 are interpreted as alluvial deposits based on the presence of horizontally laminated bedding features and well-rounded medium to coarse sandy channel sediments (Fig. 7a) in which an over-thickened Bt horizon developed during aggradation (Fig. 7b–c). These deposits are capped by either a lag channel or deflated or winnowed alluvial fan surface (Unit 3). Units 1 and 2 are culturally sterile, and Unit 3 contains only sparse and heavily-rounded artifacts within the same size grade as the surrounding clasts (Fig. 8). OSL ages dating to approximately 65 ka (LM-3161)

Table 1
Equivalent dose, dose rate and Small Aliquot (SA) OSL ages of the samples.

Sample	Depth[a] (cm)	Water content[b] (wt.%)	^{238}U (Bq kg^{-1})	^{226}Ra (Bq kg^{-1})	^{232}Th (Bq kg^{-1})	^{40}K (Bq kg^{-1})	Dry beta[c] (Gy ka^{-1})	Dry gamma[c] (Gy ka^{-1})	Cosmic ray[d] (Gy ka^{-1})	Total dose rate (Gy ka^{-1})	D_e (Gy)	OD[e] (%)	n	Age[f]
LM-3161	585	20 ± 10	10.0 ± 2.6	7.0 ± 0.3	24.1 ± 0.8	474 ± 9	1.40 ± 0.05	0.72 ± 0.01	0.08 ± 0.01	1.78 ± 0.13	118 ± 9	37	23	66 ± 7[*]
LM-3162	285	12 ± 3	8.3 ± 2.3	6.8 ± 0.3	23.6 ± 0.7	503 ± 10	1.46 ± 0.05	0.74 ± 0.01	0.13 ± 0.01	2.04 ± 0.07	174 ± 19	51	23	85 ± 10[*]
LM12-10	190	5 ± 2	13.2 ± 3.6	7.4 ± 0.4	30.2 ± 1.1	384 ± 10	1.23 ± 0.05	0.73 ± 0.01	0.15 ± 0.01	2.00 ± 0.06	95 ± 8	33	24	47 ± 4
LM12-11	160	5 ± 2	17.8 ± 4.8	12.9 ± 0.4	39.2 ± 1.1	417 ± 10	1.34 ± 0.06	0.86 ± 0.03	0.16 ± 0.02	2.36 ± 0.07	72 ± 3	15	20	30 ± 1
LM12-12	60	5 ± 2	17.6 ± 4.0	15.3 ± 0.3	42.8 ± 0.9	414 ± 8	1.45 ± 0.05	0.97 ± 0.02	0.19 ± 0.02	2.46 ± 0.07	42 ± 1	25	16	17 ± 1

[a] Depths of the samples are the vertical distance from the modern ground surface.
[b] Average water content of the samples during burial.
[c] Data from high-resolution low level gamma spectrometer were converted to infinite matrix dose rates using conversion factors given in Olley et al. (1996).
[d] Cosmic ray dose rates were calculated using the equations provided by Prescott and Hutton (1994).
[e] Over-dispersion.
[f] Central Age Model (CAM) ± 1σ error (also calculated for D_e).

Table 2
Equivalent dose and Single Grain (SG) OSL ages of the samples LM-3161 and LM-3162.

Sample	Depth[a] (cm)	Water content (wt. %)[b]	Total dose rate (Gy ka^{-1})	$D_{e,MAM}$[c] (Gy)	$D_{e,CAM}$[d] (Gy)	O.D (%)[e]	n	MAM age[f]	CAM age[g]
LM-3161	585	20 ± 10	1.78 ± 0.13	37 ± 22	113 ± 31	69	7	21 ± 12	63 ± 18
LM-3162	285	12 ± 3	2.04 ± 0.07	27 ± 4	55 ± 6	51	24	13 ± 2	27 ± 3

[*] Cosmic ray dose rates were calculated using the equations provided by Prescott and Hutton (1994) and provided in Table 1.
[a] Depths of the samples are the vertical distance from the modern ground surface.
[b] Data from high-resolution low level gamma spectrometer were converted to infinite matrix dose rates using conversion factors given in Olley et al. (1996).
[c] MAM = Minimum Age Model (Galbraith et al., 1999).
[d] CAM = Central Age Model (Galbraith et al., 1999).
[e] Over-dispersion.
[f] Minimum Age Model, ± 1σ error (4 parameters sensu Galbraith et al., 1999).
[g] Central Age Model, ± 1σ error (Galbraith et al., 1999).

were assayed from Unit 1, but authigenic mineral formation associated with groundwater fluctuations and gleying of the sediments have likely compromised the D_r estimate as demonstrated by the results of the SG OSL analysis. SA OSL and SG OSL analyses from Unit 2 (LM-3162) do not provide reliable estimates of age of deposition of this unit based on the over-dispersion values obtained.

Within Unit 4, very poorly-sorted, coarse grained alluvial fan deposits have undergone multiple phases of Bt horizon formation, which also destroyed bedding structures that may have been present (Fig. 7d–e). Artifacts (mainly unweathered and some refitting) are concentrated in the upper 10 cm of the unit, which was deposited ca. 47 ka (LM12-10; Table 1), although authigenic iron-manganese (Fe–Mn) nodule formation would have altered the dosing environment and affected the D_r over the burial life of the sample. Additionally, multiple fluctuations in moisture initiated the shrinking and swelling of smectites present in the soils, resulting in pedoturbation and the formation of vertic features (Fig. 7f–g). Vertic processes led to the physical deformation of illuvial clay coatings, but Bt horizon formation continued, as evidenced by a later phase of coatings (Fig. 7h). At one point, Bt horizon formation ceased when the groundwater table rose significantly, which gleyed much of the lower profile and contributed to the formation of Fe–Mn nodules within the inactive Bt horizon. After the groundwater level fell, the uppermost of the nodules and large clasts (including artifacts) settled downwards forming a secondary deposit of nodules in the profile, which accommodated bulk volume changes from dewatering and winnowing of fine particulates.

Following the lowering of the Fe–Mn nodule rich horizon, deposition of finer-grained, distal alluvial fan sediments recommenced prior to 30 ka (LM12-11; Table 1) and successive formation of Bt horizons continued with clay coatings forming around lower nodules (Fig 7i) and cementation from iron leaching and accumulation within the profile. Artifact counts are highest in the bottom 30 cm of Unit 5 and are virtually absent in sediments that

accumulate thereafter. Following landform stability after 17 ka (LM12-12; Table 1), lateritic soil formation pedogenically weathered quartz grains, feldspars and smectite clays top-down in Unit 5, enriching the unit in kaolinite. Additionally, termite bioturbation, associated with the formation of the laterite, occurred downwards to the top of the iron-nodule concentration (Fig. 7j).

4.2. Lithic analysis

The lithic artifacts from CHA-II form a typo-technologically generalized MSA assemblage, but provide useful data for understanding site taphonomy and land use strategies over time. Analysis of a sample of 640 piece-plotted artifacts from an area of 8 m^2 shows both dorsal and ventral sides of the artifacts were frequently coated in Fe–Mn precipitates, with only five artifacts demonstrating differential weathering on opposing sides. More detailed examination suggests that there may be two or more lenses of artifacts within this vertical concentration (Fig. 8, lower left). Vertical refits and conjoins are non-existent between designated sedimentary units. Within Unit 4 (Lower Concentration), five sets of conjoining/refitting artifacts were identified, along with eight similar sets in Unit 5 (Upper Concentration), found in discrete clusters (Fig. 9). Artifacts from CHA-II are typically more square than elongated, so that within this sample only 125 had a maximum length:breadth ratio of ≥1.5, and thus a discernable long axis. Of these, neither the upper nor the lower lens shows a preferred orientation that would suggest winnowing (McPherron, 2005). Additionally, all artifacts are lying at angles <22° (most far flatter), indicating that they have not been post-depositionally reoriented by bioturbation (Bernatchez, 2010; Lenoble and Bertran, 2004). In total, <1% of artifacts are retouched, and over 95% of cores retain some cortex coverage, with an average 44% cortex coverage on all cores.
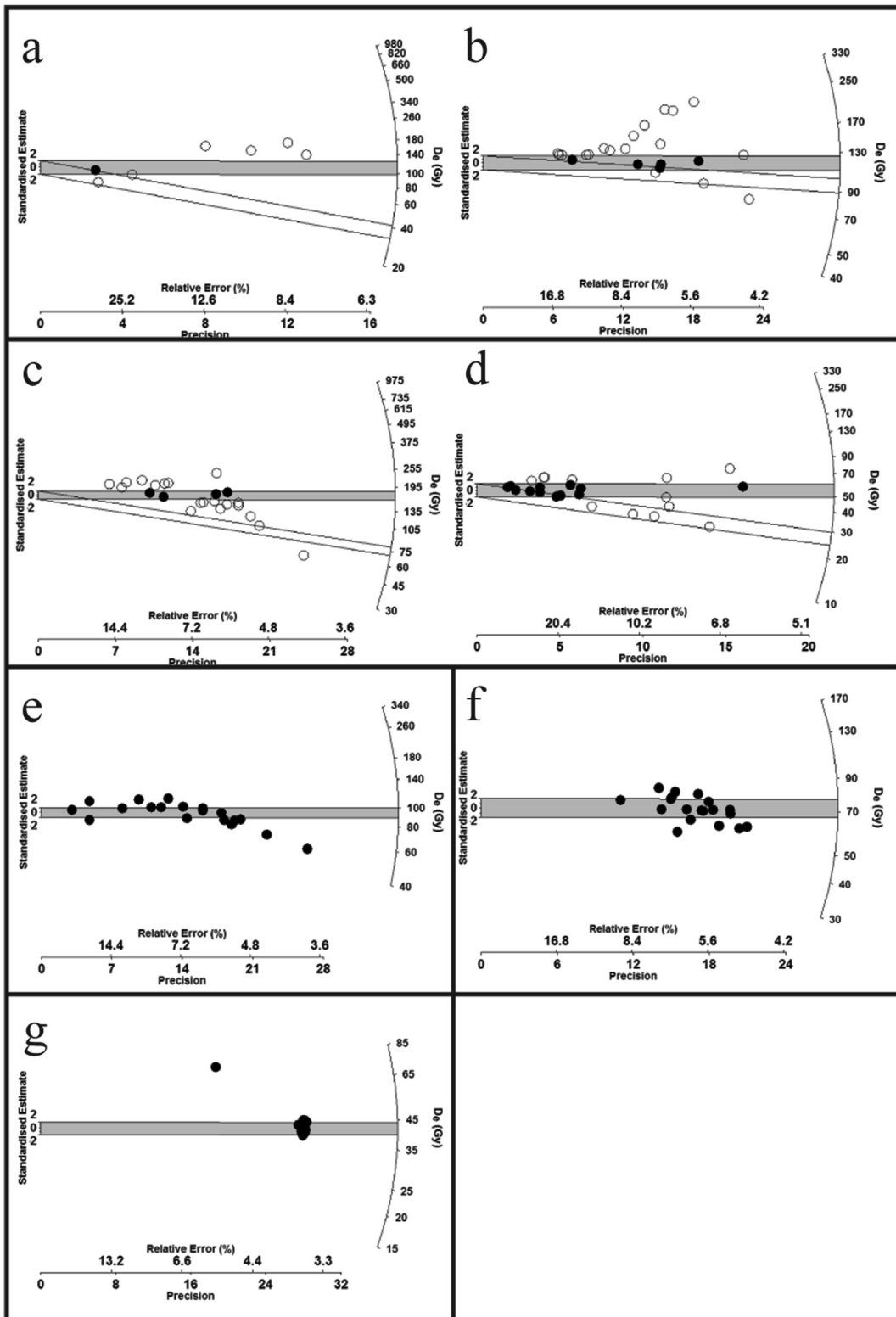
Fig. 4. Radial plots of samples from CHA-II (a) Single grain (SG) analysis of LM-3161, Central Age Model (CAM) $D_e = 113 \pm 31$ Gy, Over-dispersion (OD) = 69%, Minimum $D_e = 37 \pm 22$ Gy, CAM age = 63 ± 18 ka, Minimum age = 21 ± 12 ka; (b) Small aliquot (SA) analysis of LM-3161, CAM $D_e = 118 \pm 9$ Gy, OD = 37%, Min $D_e = 96 \pm 13$ Gy, CAM age = 66 ± 7 ka, Minimum age = 54 ± 8 ka; (c) LM-3162 (SG), CAM $D_e = 55 \pm 6$ Gy, OD = 51%, Minimum $D_e = 27 \pm 4$ Gy, CAM age = 27 ± 3 ka, Minimum age = 13 ± 2 ka; (d) LM-3162 (SA), CAM $D_e = 174 \pm 19$ Gy, OD = 51%, Minimum $D_e = 75 \pm 11$ Gy, CAM age = 85 ± 10 ka, Minimum age = 37 ± 6 ka; (e) LM12-10 (SA), CAM $D_e = 95 \pm 8$ Gy, CAM age = 47 ± 4 ka; (f) LM12-11 (SA), $D_e = 72 \pm 3$ Gy, CAM age = 30 ± 1 ka; (g) LM12-12 (SA), $D_e = 42 \pm 1$ Gy, CAM age = 17 ± 1 ka.
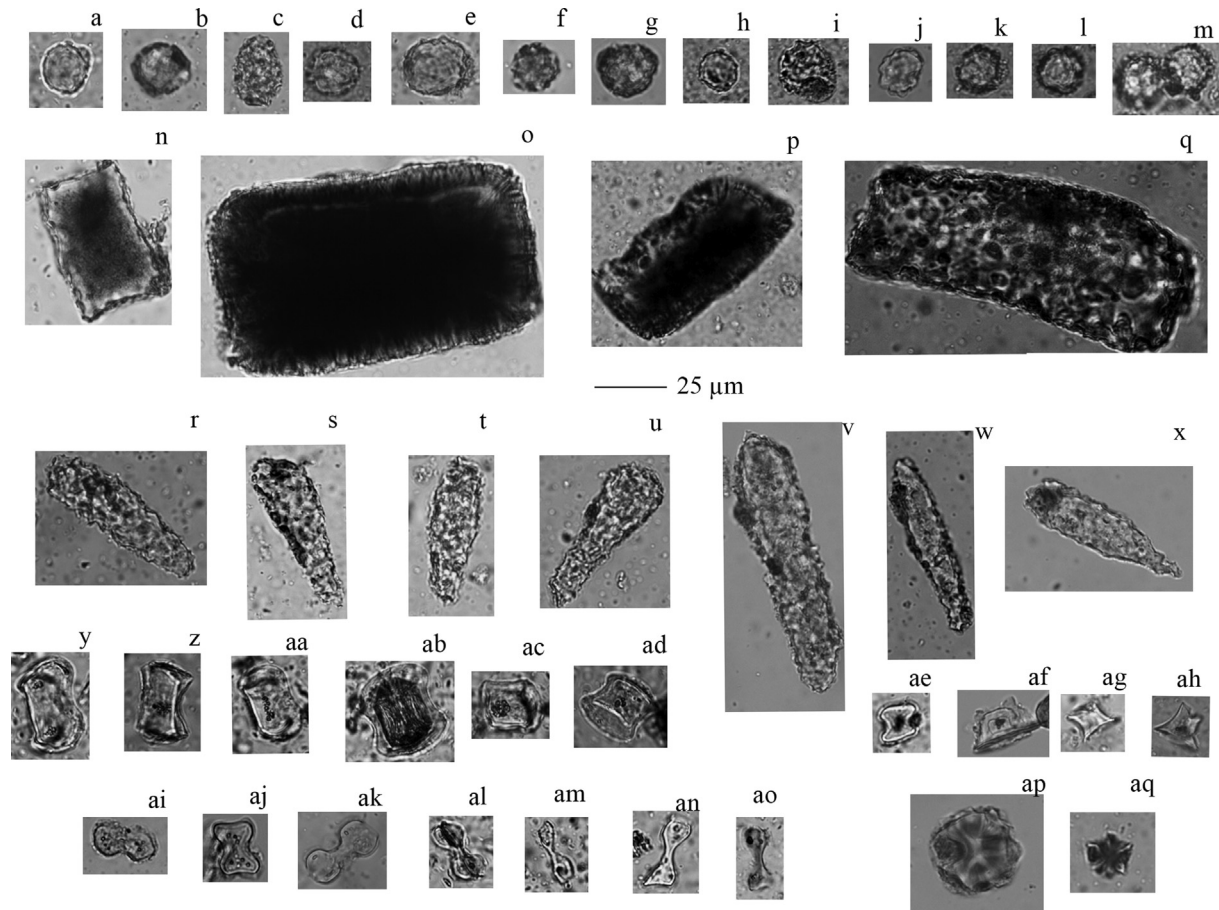
Fig. 5. Phytolith morphotypes identified from CHA-II. (a−m) globular granulates derived from dicot trees and shrubs (Mercader et al., 2009; Neumann et al., 2009; Runge, 1999); (n−q) blocky derived from arboreal taxa (Mercader et al., 2009); (r−x) clayate granulates derived from arboreal taxa (Mercader et al., 2009); (y-ad) long saddles derived from Poaceae wet-adapted bambusoids (Mercader et al., 2010; Piperno and Pearsall, 1998); (ae) short saddles derived from xeric chloridoid grasses (Mercader et al., 2010; Twiss et al., 1969); (af-ah) towers derived from xeric chloridoid grasses (Mercader et al., 2010; Twiss et al., 1969); (ai-ao) lobates derived from tall, hydric, heliophyte panicoid grasses (Barboni and Bremond, 2009; Bremond et al., 2008; Mercader et al., 2010; Novello et al., 2012); (ap-aq) globular, 'ridged' with echinoid appearance derived from the Mararantaceae family, forest-adapted taxa (de Albuquerque et al., 2013).

4.3. Phytolith analysis

Phytolith data provide an additional environmental context for the depositional and artifactual data (Supplementary Online Material 2). Phytoliths from woody (arboreal) tissue average 86.2% (range: 61.5−100%) and therefore they constitute the dominant type analyzed from CHA-II. Overall, this is indicative of a generally moist arboreal domain; however, there are cyclical peaks and drops in the abundance of arboreal phytoliths that can be classed into four vegetation phases illustrating the alternation of three wet periods with two drier ones (Fig. 6). There was no evidence for mixing of phytolith taxa between the following phases:

- 'Phase 1' is from Unit 1, and is likely much older than 47 ka and inferred to be ca. 65 ka based on SA OSL and SG OSL analyses with low confidence in the accuracy of this age estimate. The lower part of these sediments contains heavy arboreal representation, which transforms into fragmented woodland (arboreal phytoliths: 61.5%) in the upper part of Unit 1, where seasonal (panicoid) and wet-adapted (bambusoid) communities still abound (Poaceae phytoliths combined: >30%). This zone is interpreted as reflecting a wet woodland community.
- 'Phase 2' also predates 47 ka, and it yields the highest levels of arboreal phytoliths from the entire series, with grasses being minimal or absent. Phytoliths from this zone are interpreted as

reflecting a forest environment, and correspond to geologic Units 2 and 3.

- 'Phase 3' records significant arboreal reduction starting at the stratigraphic level dated to 47 ka through 30 ka, and covering the upper solum of geologic Unit 4, and lower 30 cm of Unit 5. Phytoliths from the dry-adapted chloridoid clade peak at 58.6% for all Poaceae types. This zone is interpreted as signalling the presence of predominantly dry, grassy woodland.
- 'Phase 4' postdates 30 ka and extends to <17 ka. Taxa analyzed from this zone indicate a return to arboreal dominance for the remainder of the stratigraphic column, albeit with small fluctuations in seasonal-grass types. This phase is inferred as reflecting dense woodland, which is distinct from the present-day Zambezi woodland vegetation classification of the region (White, 1983).

4.4. Comparison of CHA-II to regional paleoclimatic datasets

Terrestrial data sets present in CHA-II and other sites in the Karonga region correlate with regional climatic events documented in the Lake Malawi Drill Core and other regional proxies (Fig. 10). Terrigenous pollen consistently include miombo and bamboo forest species with some grasses throughout MIS3 (Beuning et al., 2011) with coeval supporting evidence coming
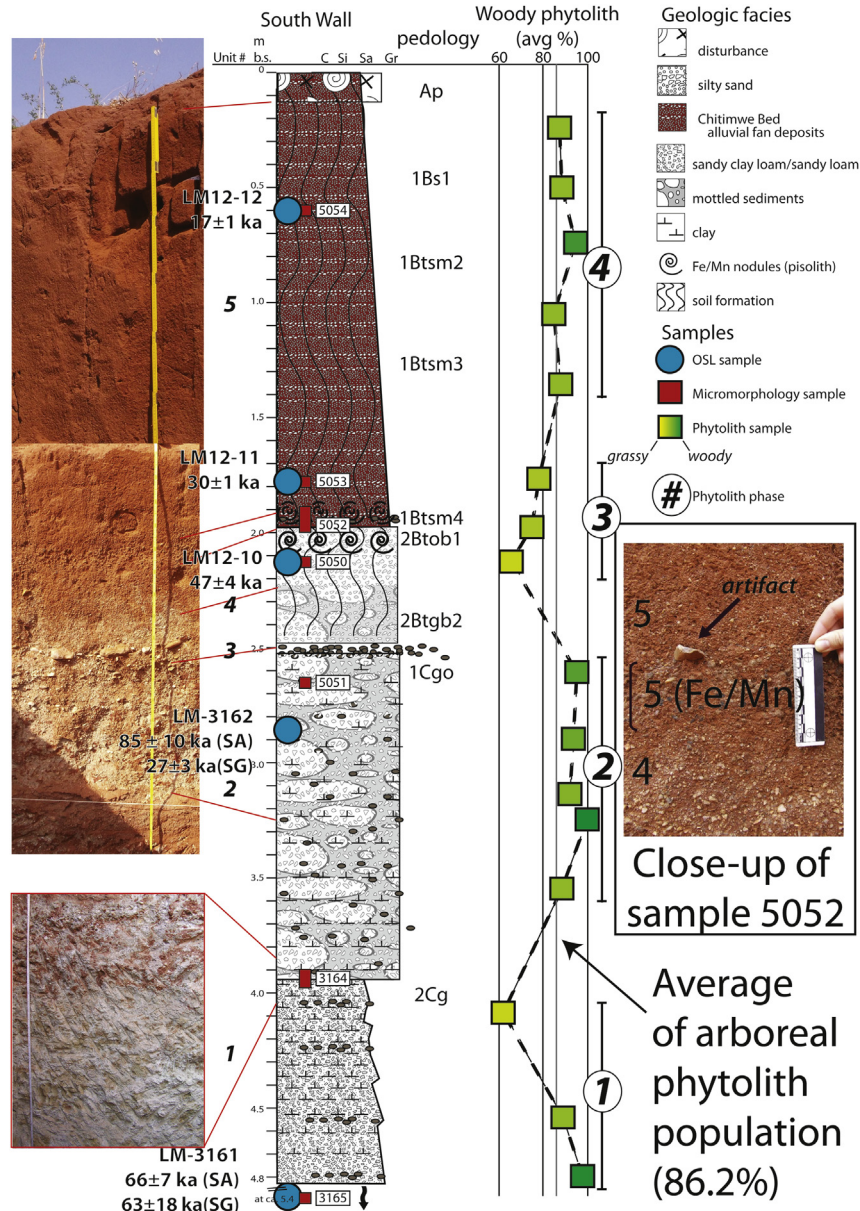
Fig. 6. South wall profile of CHA-II showing sedimentology, pedology, sampling locations and interpretation of phytolith taxa present. Sample 5052 (middle right) is shown in thin section in Fig. 7d–i and is stratigraphically associated with the densest artifact accumulations.

from phytolith assemblages on the Mozambican side of the lake (Mercader et al., 2013). However, diatom assemblages reflect shallower water conditions between 47 and 32 ka (Stone et al., 2011), concurrent with Phase 3 reductions in arboreal taxa from CHA-II. Regionally, the wettest conditions occur during the Early Holocene (Bonnefille and Chalié, 2000; Ivory et al., 2012; Stone et al., 2011; Tierney et al., 2008), which correlates with Phase 4 of the CHA-II phytolith sequence. Overall, the magnitude of lake level fluctuations during the last 60 ka in Lake Malawi was far less significant compared to nearby lakes Masoko and Tanganyika (Fig. 10), which may have made it a more attractive biome for persistent human habitation.

5. Discussion

The integrated paleoecological and archaeological

reconstructions of CHA-II were designed to maximize the information potential of an open-air MSA site in tropical Africa. Preservation of organic remains is typically poor in tropical regions, and especially so in open-air settings, and CHA-II was no exception. However, by analyzing inorganic fossil remains of plants, sediments and artifacts, MSA environments and potential drivers of human behavior can be inferred on both a local and regional level.

5.1. Depositional and age models of CHA-II

In tropical environments, where rainfall tends to be heavy and seasonal, alluvial fans are typically activated during a high precipitation event following a drought severe enough to devegetate large swaths of an upland region (e.g., Kumar Singh et al., 2001; Nott et al., 2001; Thomas, 2004; Waters et al., 2010). Tectonic activity can also catalyze alluvial fan formation, but in the absence of
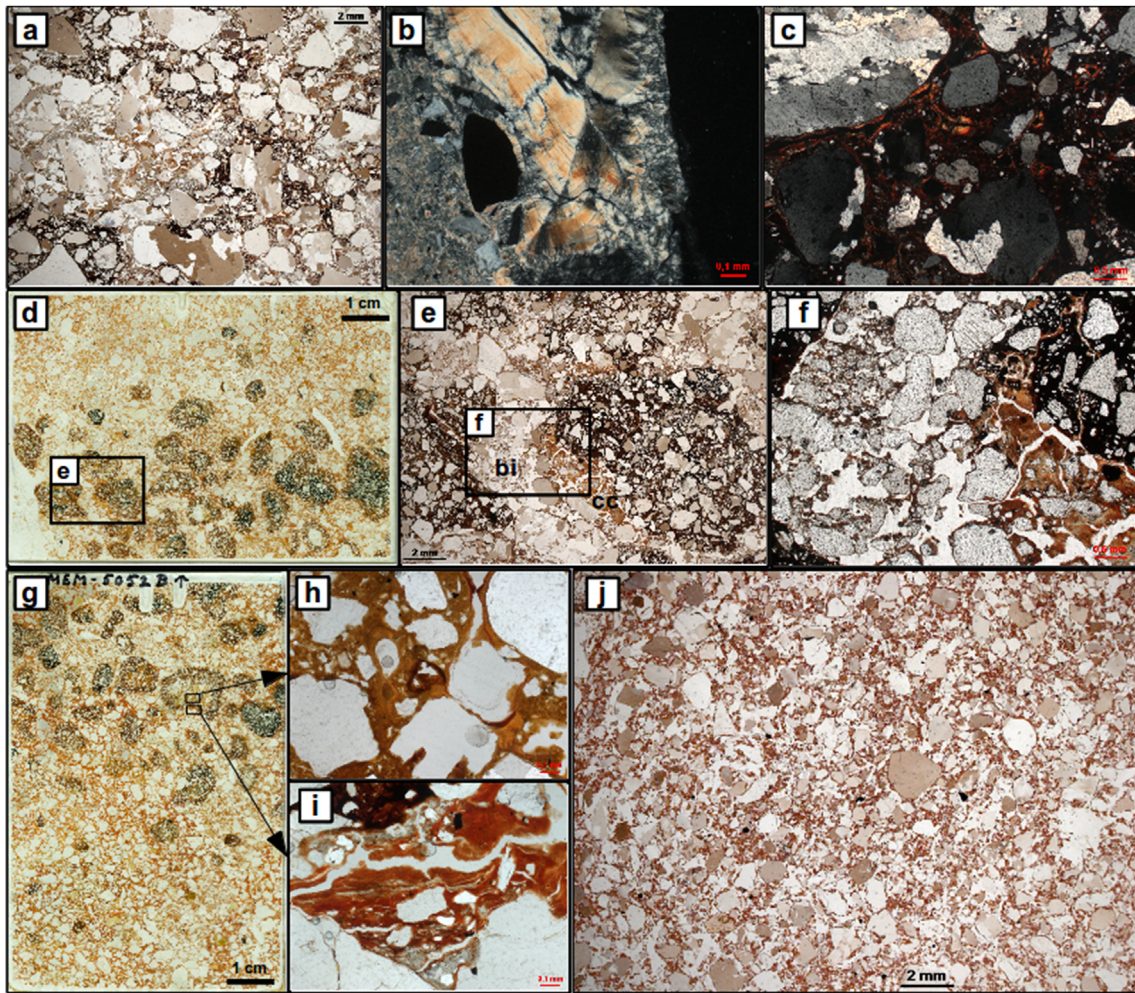
Fig. 7. Sedimentologic features of Chaminade-II through micromorphologic thin section. (a) Orthic nodules in Unit 2 underneath the concentration of iron-manganese nodules (sample MEM-5050). PPL; (b) old deformed clay coating with kink-band fabric resulting from shrink and swell (MEM-3164B). XPL; (c) fresh clay coatings from a relatively recent phase of Bt formation (MEM-5050). XPL; (d) scan of MEM-5052 thin section showing the upper half of the iron-manganese nodule concentration (6 × 9 cm); (e) anorthic iron-manganese nodules with remnants of clay coatings [c] from a Bt horizon and a bioturbated zone [bi] in between nodules. PPL; (f) framed area at higher magnification showing open bioturbated material and remnants of clay coatings on a nodule. PPL; (g) scan of thin section (6 × 9 cm) showing the lower half of the iron-manganese nodule concentration with orthic and anorthic nodules (MEM-5052B); (h) dusty clay coatings from inside an iron nodule (upper frame in [g]). Earlier phase of Bt formation pre-dating iron nodule formation; (i) iron stained clay coatings from outside an iron nodule (lower frame in [g]), representing a later phase of Bt formation, post dating iron nodule formation and deflation; (j) intergrain microaggregate microstructure, resulting from extensive termite activity in the laterite (MEM-5054). PPL.
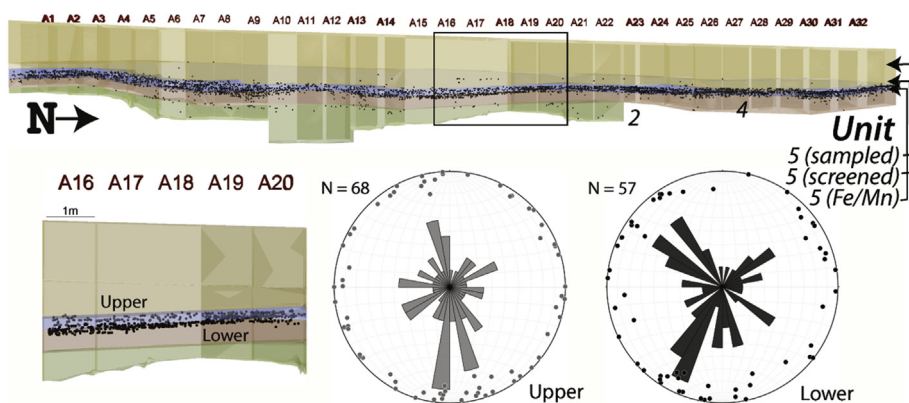
Fig. 8. CHA-II trench showing sedimentologic/pedologic units and locations of plotted finds (black points). Note that artifacts in the upper portion of Unit 5 were not piece-plotted, but that sieving showed they averaged <1/m³. A close-up of squares A16-B20 is shown at lower left, with only artifacts in the main concentration pictured for clarity. These have been divided into two possible lenses, with a separate rose diagram at lower right given for each. The points on the rose diagrams represent the plunge of the artifacts, while the roses themselves represent their orientations.
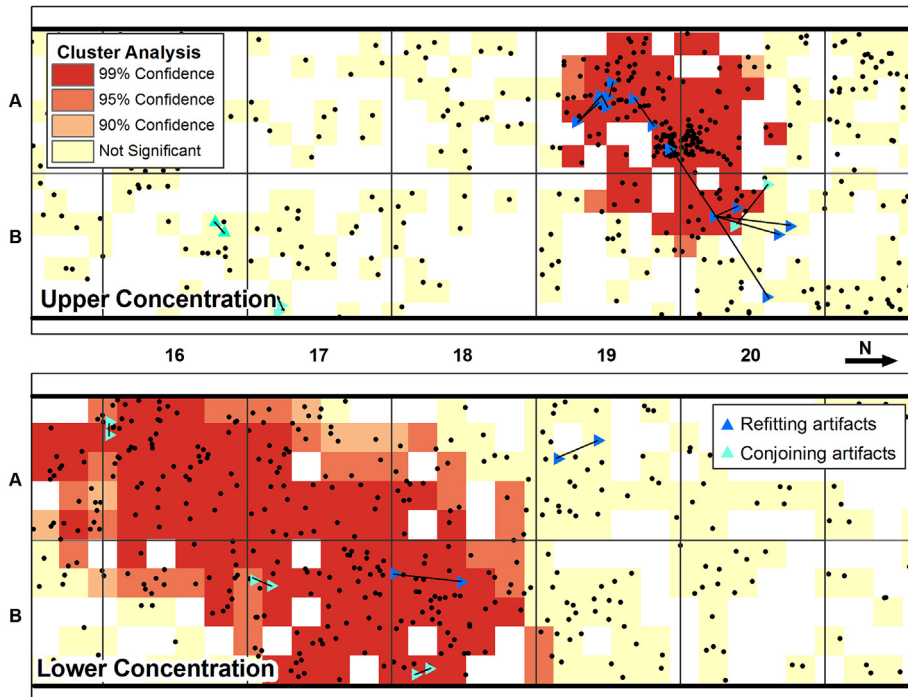
Fig. 9. Results of refitting program and GIS cluster analysis. Following Sisk and Shea (2008), "refits" are artifacts that were separated through the knapping process/conchoidal fracturing, while "conjoins" are fragments of formerly whole flakes that fit back together. In both the Upper and Lower Concentrations, refitting and conjoining artifact sets occur predominantly within cluster of artifacts identified using the Optimized Hot Spot Analysis functionality in ArcGIS 10.2. This tool identifies spatially concentrated incidences (of artifacts), and identifies the likelihood that the spatial relationships within them reject the null hypothesis of a random distribution, at increasing confidence levels.

significant upwarping or solifluction alluvial fan formation normally occurs in tandem with variable precipitation (e.g., Bull, 1977; Harvey, 2002; Kumar et al., 2007; Ritter et al., 1995; Wang et al., 2001). Erosional and depositional processes across alluvial fans are not uniform and sheetwash zones, channels and debris flows are distributed irregularly across landforms (see papers in Harvey et al., 2005 for a comprehensive review).

Based on the available evidence, sedimentation of CHA-II occurred primarily as pulses of distal alluvial fan deposits, which were sometimes reworked and deposited by intermittently occurring fluvial systems (Fig. 11). Sediment packages were poorly sorted, well mixed and do not appear to vary appreciably over the 32 m exposed length of the site. Clast sizes generally range between fine and coarse sand with pockets of sediments with higher gravel fraction.

The potential for large-scale bioturbation at CHA-II is high, but the evidence suggests that such activity was localized. Groundwater fluctuations and lateritic processes facilitated the formation of the Fe—Mn nodule-rich lens that overprints bedding features from the upper portion of the sondage. Subsidence from water table depletion has been observed at CHA-II based on the uniform, undulating sediment packages observable in the profile (Fig. 8), but large accommodation zones for fine clasts to move downward do not appear to have formed. Conjoins and refits from Units 4 and 5 (Fig. 9) and clusters of chipped stone debris indicate that these are primary or minimally compressed archaeological deposits reflecting discrete activity areas. Furthermore, the micromorphology indicates that sediment mixing was restricted to distinct sedimentary zones and large-scale lateral movement of sediments decimeters from their primary depositional environment was not significant.

In addition to being a tool for dating sediment deposition, OSL is commonly used as a tool to understand bioturbation and pedoturbation within archaeological contexts (e.g., Arnold and Roberts,

2009; Gliganic et al., 2012; Guérin et al., 2015). Because the sedimentary matrix reworking at CHA-II was localized, SA OSL was employed as the method of first resort. Recent studies demonstrate that if over-dispersion is within a threshold range of <40%, it is possible to obtain accurate age estimates from SA OSL analysis as long as the skewness values within a population of aliquots are low indicating a normal or log normal distribution (Alexanderson and Murray, 2007; Armitage and King, 2013; Arnold and Roberts, 2009; Forman, 2015; Rowan et al., 2012). Radial plots of samples from CHA-II demonstrate a central tendency of the aliquots with the exceptions of LM-3161 and LM-3162 (Fig. 4), which show scattered D_e values indicating some sediment reworking, pedoturbation and non-solar resetting of sediments prior to deposition. Based on the combined evidence, one age is rejected (LM-3161) and two ages are considered highly uncertain (LM-3162 and LM12-10), however post-depositional effects did not significantly impact the accuracy of LM12-11 and LM12-12.

The combined sedimentary, micromophological, artifactual, phytolith, and OSL data infer a depositional model that is inconsistent with Crossley (1986) interpretation of site taphonomies from the Chitimwe Beds. Based on granulometric analyses of the sand sheets and termite mounds in the Chaminade area, Crossley (1986) concluded that the vertical (upward) transfer of selected (medium to coarse) sand grains by *Macrotermes falciger* termites led to the accumulation of the sand sheets and concentration of larger particles and lithic artifacts in the lower reaches of the solum. Instead, we argue that Bt horizon overthickening and the formation of vertic features associated with soil formation and groundwater variability degraded the integrity of bedding features in the profile commonly found in alluvial deposits, making the deposits appear similar to biomantles to the naked eye.
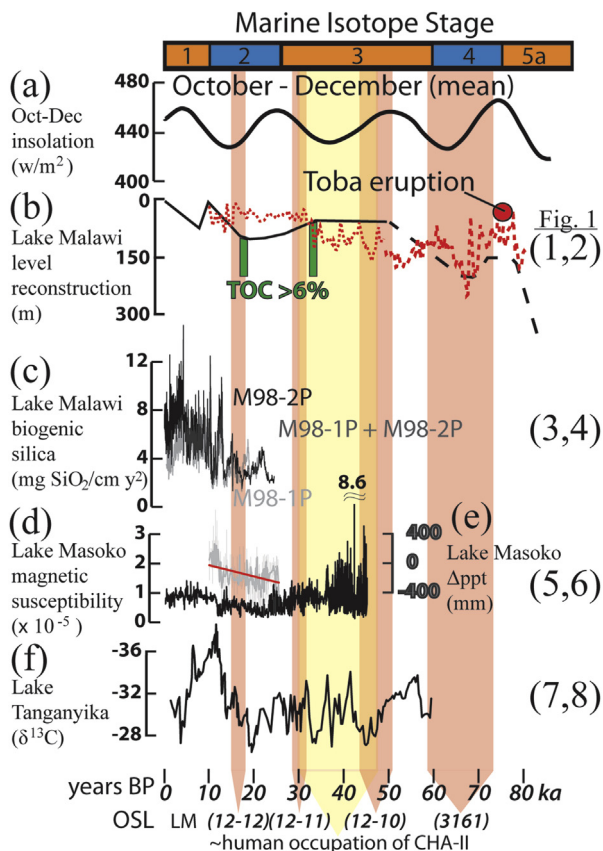
Fig. 10. Paleoclimatic proxy data from southeastern Africa. (a) Average insolation (w/m²) at the onset of the rainy season (October–December) at 10°S (Scholz et al., 2011); (b) Black line is the interpreted lake level based on synthesis of sediment core data (Scholz et al., 2011), red dotted line is a reconstructed lake level based on the diatom assemblage from the Lake Malawi Drill Cores (Stone et al., 2011), dashed lines after 50 ka represent age model uncertainty from discovery of Toba Ash as reported in Lane et al. (2013); (c) Biogenic silica mass accumulation rate (mg SiO₂/cm y²) from Lake Malawi (Johnson et al., 2002); (d) Magnetic susceptibility (×10⁻⁵) from Lake Masoko (Garcin et al., 2006); (e) Gray line shows Δppt from modern conditions (mm) from Lake Tanganyika, red line shows time-averaged linear trendline (Bonnefille and Chalié, 2000); (f) δ¹³C of monocarboxylic fatty acids (C₂₈) vs. VPDB from Lake Tanganyika (Tierney et al., 2008). Numbers on right margin correspond to proxy points identified in Fig. 1. (For interpretation of the references to color in this figure legend, the reader is referred to the web version of this article.)

5.2. Landscape and behavioral models of CHA-II

Archaeological evidence from CHA-II records recurrent occupation associated with MSA foragers throughout the late MIS4 and entire MIS3 periods in the Karonga region. Diatom and geochemical proxy reconstructions of the Lake Malawi ecology indicate that site sedimentation occurs when the local environment fluctuates between mildly xeric and pluvial conditions (Finney et al., 1996; Gasse et al., 2002; Stone et al., 2011). The diatom assemblage from Lake Malawi following the eruption of Mount Toba (ca. 75 ka) and prior to 50 ka shows several prominent and rapid ecological changes (Lane et al., 2013; Stone et al., 2011), which broadly accord with the phytolith assemblage from Units 1 and 2 of CHA-II. Similarly, phytolith taxa from CHA-II connote the presence of dry, grassy woodland from this time, which are echoed in the reconstructed paleoenvironments of the Mozambican highlands for the interval 50 to >42ka (Mercader et al., 2013: 330). Phytoliths entrained in Units 1–3 reflect the predominance of wet woodland to forest environments, indicative of a moist precipitation regime during periods of site sedimentation. Proportions of woody vegetation

drop markedly in Unit 4, which was filled by alluvial fan deposits, and then increase again through Unit 5. Occurrences of the MSA in the area are inferred prior to 47 ka by the presence of heavily-rolled artifacts in deposits associated with Unit 3 and the bottom of Unit 4.

Human occupation at the site began in earnest after 47 ka and appears to have occurred during a period of profound landscape variability. Based on magnetic susceptibility of an assayed lake core at Lake Masoko (Fig. 10d), located 70 km to the north of CHA-II, the region experienced longer dry seasons and potentially stronger seasonality in precipitation compared to present conditions, but was dominated by Zambezian tree, open savannah vegetation (Garcin et al., 2006). Similarly, the environment at CHA-II became more open, which is supported by on-site grassy phytoliths and off-site diatom data from Lake Malawi reflecting higher alkalinity (Stone et al., 2011). After 30 ka, the phytolith spectra at CHA-II reflect the presence of a dense woodland community, which is in agreement with pollen and biogenic silica data derived from the Lake Malawi sediment core (Beuning et al., 2011; Johnson et al., 2011; Stone et al., 2011) and Lake Masoko (Garcin et al., 2006).

The concentration of artifacts within Unit 5 is the product of repeated occupation of the same land surface as soil aggraded over an extended period of time concurrent with slow sedimentation of the landform prior to 30 ka as the climate transitioned to wetter conditions (Fig. 11). Toolstone types and limited reduction of nodules indicate that toolstone availability was not a limiting factor. Rather, MSA foraging strategies incorporated regular visits to riparian zones for lithic raw material, which was processed and then transported outside the riparian areas for usage. Similar patterns of landscape utilization within diagenetically-altered alluvial fan sedimentary environments have been documented in the Kapthurin Formation (Tryon, 2010) and Mukogodo Hills (Pearl and Dickson, 2004) of Kenya and Jebel Gharbi in north-west Libya (Barich et al., 2006) possibly representing a generalized site taphonomy and behavioral strategy of MSA foragers operating in dynamic sedimentary and climatic environments. Artifacts entrained above the lower 30 cm of Unit 5 are relatively rare and likely bioturbated within the sediments either through termite activity or entrainment in the alluvial fan. Some artifacts from the upper portions of Unit 5, including some small pieces, can be characterized as Later Stone Age (LSA), whereas none from within the zone of artifact concentration can be assigned firmly to any typo-technological complex other than the MSA. This adherence to cultural stratigraphy provides additional support for our interpretation of the site's formation (Fig. 11).

The micro-scale data are corroborated by lithic orientation data at CHA-II, which show most artifacts as lying horizontally, and by the lack of mixing of small LSA elements into the sediments dated >30 ka. This demonstrates that MSA behavior at both site and landscape scales can still be discerned in tropical settings that have been subsequently affected by tectonic, authigenic, pedogenic and climatic changes since the times of original artifact deposition.

6. Conclusion

Archaeological research of MSA occupation of CHA-II located on an alluvial fan in northern Malawi integrated paleoclimatologic, sedimentologic and spatial datasets to better understand human habitation patterns within a tropical to subtropical ecosystem. The primary human occupation of the landform occurred between 47 and 30 ka, concentrated on slowly aggrading alluvial fan sediments within a grassy woodland zone that was drier than during preceding and following phases of sedimentation. Although this is the driest period reflected in diatom assemblages after 70 ka (Stone et al., 2011), the magnitude of ecological variability in Lake Malawi appears to have been far less than in surrounding basins at
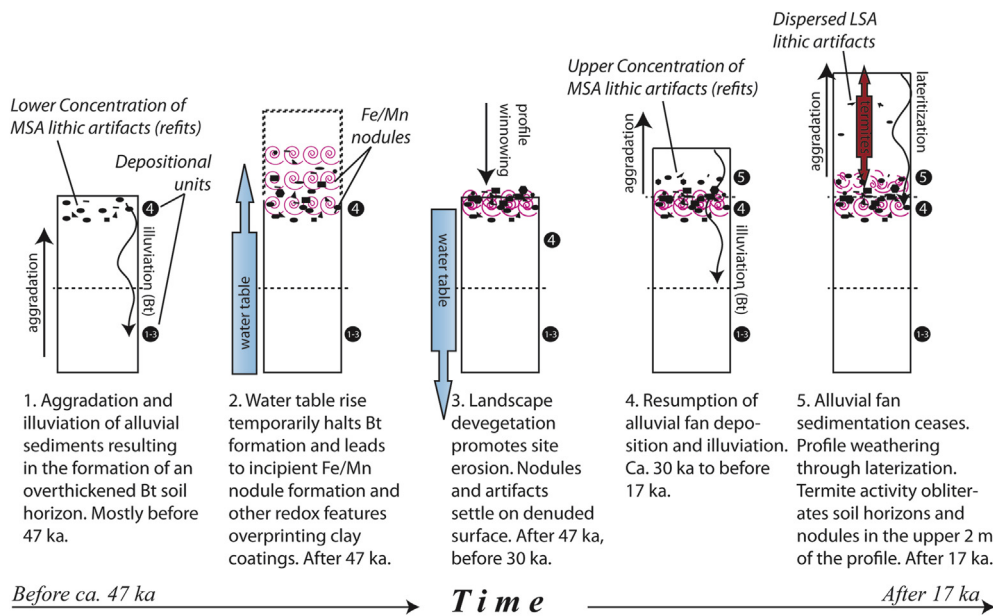
Fig. 11. Site formation model for Chaminade-II.

the same time (Bonnefille and Chalié, 2000; Tierney et al., 2008). The evidence for repeated visits to the site and lack of conservation of toolstone suggests that this was a relatively attractive environment for MSA foragers. CHA-II demonstrates similar patterns in landform utilization to other MSA sites in the Karonga region (Thompson et al., 2012; Wright et al., 2014), on the Mozambican side of the lake (Bicho et al., (in press); Mercader et al., 2011, 2013) and elsewhere in Africa as cited above.

The taphonomic situation at CHA-II and other sites did not allow for the preservation of evidence for other human activities such as faunal resource exploitation or hearth construction. Much archaeology conducted in tropical ecosystems faces similar challenges due to generally poor preservation conditions in biomes with high, seasonal rainfall and rapid soil formation. Bioturbation from insects tends to be particularly severe due to the lack of cold conditions to seasonally limit tunnel construction activities. Laterite formation and highly acidic soils also degrade the integrity of organic deposits and buried A-horizons, as does redoximorphic weathering of sediments associated with fluctuating ground water levels. More specifically to the MSA, the lack of diversity in the material culture, particularly from open-air settings, limits behavioral interpretations (Sharon et al., 2014).

In spite of these limitations, archaeological studies of open-air MSA sites from tropical regions are critical for developing robust models explaining human behavioral evolution and diversity (Shea, 2011). Therefore, we advocate a multiproxy, multidisciplinary research strategy that can sufficiently tackle the challenges of working in tropical ecosystems and yield information needed to contribute to such discussions. This study shows that detailed information about MSA landscape use, lithic exploitation, and local environments can be reconstructed using multiple lines of evidence tailored to these challenging preservation conditions. Furthermore, regional paleoecological datasets augment site-scale archaeology and sedimentology, providing a broader context for deposition, soil formation and aspects of human behavior.

Appendix A. Supplementary data

Supplementary data related to this article can be found at http://dx.doi.org/10.1016/j.jas.2016.01.014.

References

Ahr, S.W., Nordt, L.C., Driese, S.G., 2012. Assessing lithologic discontinuities and parent material uniformity within the Texas sandy mantle and implications for archaeological burial and preservation potential in upland settings. Quat. Res. 78, 60–71.

Albert, R.M., Bamford, M.K., Cabanes, D., 2009. Palaeoecological significance of palms at Olduvai Gorge, Tanzania, based on phytolith remains. Quat. Int. 193, 41–48.

Alexanderson, H., Murray, A.S., 2007. Was southern Sweden ice free at 19-25 ka, or were the post LGM glacifluvial sediments incompletely bleached? Quat. Geochronol. 2, 229–236.

Araujo, A.G.M., 2013. Bioturbation and the upward movement of sediment particles and archaeological materials: comments on Bueno et al. J. Archaeol. Sci. 40, 2124–2127.

Armitage, S.J., King, G.E., 2013. Optically Stimulated Luminescence dating of hearths from the Fazzan Basin, Libya: a tool for determining the timing and pattern of Holocene occupation of the Sahara. Quat. Geochronol. 15, 88–97.

Arnold, L.J., Roberts, R.G., 2009. Stochastic modelling of multi-grain equivalent dose (De) distributions: Implications for OSL dating of sediment mixtures. Quat. Geochronol. 4, 204–230.

Barboni, D., Bremond, L., 2009. Phytoliths of East African grasses: an assessment of their environmental and taxonomic significance based on floristic data. Rev. Palaeobot. Palynol. 158, 29–41.

Barich, B.E., Garcea, E.A.A., Giraudi, C., 2006. Between the Mediterranean and the Sahara: geoarchaeological reconnaissance in the Jebel Gharbi, Libya. Antiquity 80, 567–582.

Beauvais, A., Bertaux, J., 2002. In situ characterization and differentiation of kaolinites in lateritic weathering profiles using infrared microspectroscopy. Clays Clay Miner. 50, 314–330.

Bernatchez, J.A., 2010. Taphonomic implications of orientation of plotted finds from Pinnacle Point 13B (Mossel Bay, western Cape Province, South Africa). J. Hum. Evol. 59, 274–288.

Betzler, C., Ring, U., 1995. Sedimentology of the Malawi Rift: facies and stratigraphy of the Chiwondo Beds, northern Malawi. J. Hum. Evol. 28, 23–35.

Beuning, K.R.M., Zimmerman, K.A., Ivory, S.J., Cohen, A.S., 2011. Vegetation response to glacial–interglacial climate variability near Lake Malawi in the southern African tropics. Palaeogeogr. Palaeoclimatol. Palaeoecol. 303, 81–92.

Bicho, N., Haws, J., Raja, M., Madime, O., Gonçalves, C., Cascalheira, J., Benedetti, M., Pereira, T., Aldeias, V., 2015. Middle and Late Stone Age of the Niassa region, northern Mozambique. Preliminary results. Quaternary International (in press), http://dx.doi.org/10.1016/j.quaint.2015.09.059.

Bonnefille, R., Chalié, F., 2000. Pollen-inferred precipitation time-series from Equatorial mountains, Africa, the last 40 kyr BP. Glob. Planet. Change 26, 25–50.

Bremond, L., Alexandre, A., Wooller, M.J., Hély, C., Williamson, D., Schäfer, P.A., Majule, A., Guiot, J., 2008. Phytolith indices as proxies of grass subfamilies on East African tropical mountains. Glob. Planet. Change 61, 209–224.

Brown, K.S., Marean, C.W., Jacobs, Z., Schoville, B.J., Oestmo, S., Fisher, E.C., Bernatchez, J., Karkanas, P., Matthews, T., 2012. An early and enduring advanced technology originating 71,000 years ago in South Africa. Nature 491, 590–593.

Bull, W.B., 1977. The alluvial-fan environment. Prog. Phys. Geogr. 1, 222–270.

Clark, J.D., Haynes, C.V., 1970. An elephant butchery site at Mwanganda's Village, Karonga, Malawi, and its relevance for Palaeolithic archaeology. World Archaeol. 1, 390–411.

Clark, J.D., Haynes, C.V., Mawby, J.E., Gautier, A., 1970. Interim report on palaeoanthropological investigations in the Lake Malawi Rift. Quaternaria 13, 305–354.

Clark, J.D., Stephens, E.A., Coryndon, S.C., 1966. Pleistocene fossiliferous lake beds of the Malawi (Nyasa) Rift: a preliminary report. Am. Anthropol. 68, 46–87.

Cohen, A., Stone, J.R., Beuning, K.R.M., Park, L.E., Rainthal, P.N., Dettman, D., Scholz, C.A., Johnson, T.C., King, J.W., Talbot, M.R., Brown, E.T., Ivory, S.J., 2007. Ecological consequences of early Late Pleistocene megadroughts in tropical Africa. Proc. Natl. Acad. Sci. 104, 16422–16427.

Conard, N., 2015. Cultural evolution during the Middle and Late Pleistocene in Africa and Eurasia. In: Henke, W., Tattersall, I. (Eds.), Handbook of Paleoanthropology. Springer Berlin Heidelberg, pp. 2465–2508.

Courty, M.-A., Goldberg, P., Macphail, R., 1989. Soils and Micromorphology in Archaeology. Cambridge University Press, Cambridge, UK.

Crossley, R., 1984. Controls of sedimentation in the Malawi Rift Valley, Central Africa. Sediment. Geol. 40, 33–50.

Crossley, R., 1986. Sedimentation by Termites in the Malawi Rift Valley. Geological Society, London, pp. 191–199. Special Publications 25.

d'Errico, F., Stringer, C.B., 2011. Evolution, revolution or saltation scenario for the emergence of modern cultures? Philos. Trans. R. Soc. B Biol. Sci. 366, 1060–1069.

d'Errico, F., Vanhaeren, M., Barton, N., Bouzouggar, A., Mienis, H., Richter, D., Hublin, J.-J., McPherron, S.P., Lozouet, P., 2009. Additional evidence on the use of personal ornaments in the Middle Paleolithic of North Africa. Proc. Natl. Acad. Sci. 106, 16051–16056.

de Albuquerque, E., Braga, J., Vieira, R., 2013. Morphological characterisation of silica phytoliths in Neotropical Marantaceae leaves. Plant Syst. Evol. 299, 1659–1670.

Downs, R.T., 2006. The RRUFF Project: an integrated study of the chemistry, crystallography, Raman and infrared spectroscopy of minerals. In: 19th General Meeting of the International Mineralogical Association, Kobe, Japan.

Duller, G.A.T., 2003. Distinguishing quartz and feldspar in single grain luminescence measurements. Radiat. Meas. 37, 161–165.

Ebinger, C.J., Deino, A.L., Tesha, A.L., Becker, T., Ring, U., 1993. Tectonic controls on rift basin morphology: evolution of the northern Malawi (Nyasa) Rift. J. Geophys. Res. Solid Earth 98, 17821–17836.

Eren, M.I., Durant, A.J., Prendergast, M., Mabulla, A.Z.P., 2014. Middle Stone Age archaeology at Olduvai Gorge, Tanzania. Quat. Int. 322–323, 292–313.

Feathers, J.K., 2002. Luminescence dating in less than ideal conditions: case studies from Klasies River main site and Duinefontein, South Africa. J. Archaeol. Sci. 29, 177–194.

Fernández Honaine, M., Zucol, A.F., Osterrieth, M.L., 2009. Phytolith analysis of Cyperaceae from the Pampean region, Argentina. Aust. J. Bot. 57, 512–523.

Finney, B.P., Scholz, C.A., Johnson, T.C., Trumbore, S., 1996. Late Quaternary lake-level changes of Lake Malawi. In: Johnson, T.C., Odada, E.O. (Eds.), The Limnology, Climatology, and Paleoclimatology of the East African Lakes. Gordon and Breach Publishers, Amsterdam, pp. 495–508.

Forman, S.L., 2015. Episodic eolian sand deposition in the past 4000 years in Cape Cod National Seashore, Massachusetts, USA in response to possible hurricane/storm and anthropogenic disturbances. Front. Earth Sci. 3. http://dx.doi.org/10.3389/feart.2015.00003.

Galbraith, R.F., Roberts, R.G., 2012. Statistical aspects of equivalent dose and error calculation and display in OSL dating: an overview and some recommendations. Quat. Geochronol. 11, 1–27.

Galbraith, R.F., Roberts, R.G., Laslett, G.M., Yoshida, H., Olley, J.M., 1999. Optical dating of single and multiple grains of quartz from jinmium rock shelter, northern Australia, part 1, Experimental design and statistical models. Archaeometry 41, 339–364.

Garcin, Y., Vincens, A., Williamson, D., Guiot, J., Buchet, G., 2006. Wet phases in tropical southern Africa during the last glacial period. Geophys. Res. Lett. 33, L07703.

Gasse, F., Barker, P., Johnson, T.C., 2002. A 24,000 yr diatom record from the northern basin of Lake Malawi. In: Odada, E.O., Olago, D.O. (Eds.), The East African Great Lakes: Limnology. Paleolimnology and Biodiversity. Kluwer Academic Publishers, Dordrecht, The Netherlands, pp. 393–414.

Gibert, E., Bergozoni, L., Massault, M., Williamson, D., 2002. AMS-C-14 chronology of 40.0 cal ka BP continuous deposits from a crater lake (Lake Massoko, Tanzania)—modern water balance and environmental implications. Palaeogeogr. Palaeoclimatol. Palaeoecol. 187, 307–322.

Gliganic, L.A., Jacobs, Z., Roberts, R.G., Domínguez-Rodrigo, M., Mabulla, A.Z.P., 2012. New ages for Middle and Later Stone Age deposits at Mumba Rockshelter, Tanzania: Optically Stimulated Luminescence dating of quartz and feldspar grains. J. Hum. Evol. 62, 533–547.

Grace, J., José, J.S., Meir, P., Miranda, H.S., Montes, R.A., 2006. Productivity and carbon fluxes of tropical savannas. J. Biogeogr. 33, 387–400.

Guérin, G., Jain, M., Thomsen, K.J., Murray, A.S., Mercier, N., 2015. Modelling dose rate to single grains of quartz in well-sorted sand samples: the dispersion arising from the presence of potassium feldspars and implications for Single Grain OSL dating. Quat. Geochronol. 27, 52–65.

Harvey, A.M., 2002. The role of base-level change in the dissection of alluvial fans: case studies from southeast Spain and Nevada. Geomorphology 45, 67–87.

Harvey, A.M., Mather, A.E., Stokes, M., 2005. Alluvial Fans: Geomorphology, Sedimentology, Dynamics. Geological Society, London, pp. 1–7. Special Publications 251, London.

Henshilwood, C.S., d'Errico, F., van Niekerk, K.L., Coquinot, Y., Jacobs, Z., Lauritzen, S.-E., Menu, M., García-Moreno, R., 2011. A 100,000-year-old ochre-processing workshop at Blombos Cave, South Africa. Science 334, 219–222.

Ivory, S.J., Lézine, A.-M., Vincens, A., Cohen, A.S., 2012. Effect of aridity and rainfall seasonality on vegetation in the southern tropics of East Africa during the Pleistocene/Holocene transition. Quat. Res. 77, 77–86.

Johnson, D.L., Domier, J.E.J., Johnson, D.N., 2005. Reflections on the nature of soil and its biomantle. Ann. Assoc. Am. Geogr. 95, 11–31.

Johnson, T.C., Brown, E.T., McManus, J., Barry, S., Barker, P., Gasse, F., 2002. A high-resolution paleoclimate record spanning the past 25,000 Years in southern East Africa. Science 296, 113–132.

Johnson, T.C., Brown, E.T., Shi, J., 2011. Biogenic silica deposition in Lake Malawi, East Africa over the past 150,000-0 years. Palaeogeogr. Palaeoclimatol. Palaeoecol. 303, 103–109.

Kaufulu, Z.M., 1983. The Geological Context of Some Early Archaeological Sites in Kenya, Malawi and Tanzania: Microstratigraphy, Site Formation and Interpretation. Department of Anthropology. University of California, Berkeley, Berkeley, p. 340.

Kaufulu, Z.M., 1990. Sedimentary environments at the Mwanganda site, Malawi. Geoarchaeol. 5, 15–27.

Kottek, M., Grieser, J., Beck, C., Rudolf, B., Rubel, F., 2006. World map of the Köppen-Geiger climate classification updated. Meteorol. Z. 15, 259–263.

Kumar, R., Suresh, N., Sangode, S.J., Kumaravel, V., 2007. Evolution of the Quaternary alluvial fan system in the Himalayan foreland basin: Implications for tectonic and climatic decoupling. Quat. Int. 159, 6–20.

Kumar Singh, A., Parkash, B., Mohindra, R., Thomas, J.V., Singhvi, A.K., 2001. Quaternary alluvial fan sedimentation in the Dehradun Valley Piggyback Basin, NW Himalaya: tectonic and palaeoclimatic implications. Basin Res. 13, 449–471.

Lane, C.S., Chorn, B.T., Johnson, T.C., 2013. Ash from the Toba supereruption in Lake Malawi shows no volcanic winter in East Africa at 75 ka. Proc. Natl. Acad. Sci. 110, 8025–8029.

Lenoble, A., Bertran, P., 2004. Fabric of Palaeolithic levels: methods and implications

for site formation processes. J. Archaeol. Sci. 31, 457–469.

Linstädter, J., Eiwanger, J., Mikdad, A., Weniger, G.-C., 2012. Human occupation of Northwest Africa: a review of Middle Palaeolithic to Epipalaeolithic sites in Morocco. Quat. Int. 274, 158–174.

Lombard, M., 2011. Quartz-tipped arrows older than 60 ka: further use-trace evidence from Sibudu, KwaZulu-Natal, South Africa. J. Archaeol. Sci. 38, 1918–1930.

Mackay, A., 2008. A method for estimating edge length from flake dimensions: use and implications for technological change in the southern African MSA. J. Archaeol. Sci. 35, 614–622.

McBrearty, S., 1990. Consider the humble termite: termites as agents of post-depositional disturbance at African archaeological sites. J. Archaeol. Sci. 17, 111–143.

McBrearty, S., Brooks, A.S., 2000. The revolution that wasn't: a new interpretation of the origin of modern human behavior. J. Hum. Evol. 39, 453–563.

McPherron, S.J.P., 2005. Artifact orientations and site formation processes from total station proveniences. J. Archaeol. Sci. 32, 1003–1014.

Mercader, J., Astudillo, F., Barkworth, M., Bennett, T., Esselmont, C., Kinyanjui, R., Grossman, D.L., Simpson, S., Walde, D., 2010. Poaceae phytoliths from the Niassa Rift, Mozambique. J. Archaeol. Sci. 37, 1953–1967.

Mercader, J., Bennett, T., Esselmont, C., Simpson, S., Walde, D., 2009. Phytoliths in woody plants from the miombo woodlands of Mozambique. Ann. Bot. 104, 91–113.

Mercader, J., Bennett, T., Esselmont, C., Simpson, S., Walde, D., 2011. Soil phytoliths from miombo woodlands in Mozambique. Quat. Res. 75, 138–150.

Mercader, J., Bennett, T., Esselmont, C., Simpson, S., Walde, D., 2013. Phytoliths from Middle Stone Age habitats in the Mozambican Rift (105–29 ka). J. Hum. Evol. 64, 328–336.

Mercader, J., Marti, R., Gonzalez, I.J., Sanchez, A., Garcia, P., 2003. Archaeological site formation in rain forests: insights from the Ituri rock shelters, Congo. J. Archaeol. Sci. 30, 45–65.

Murray, A.S., Wintle, A.G., 2000. Luminescence dating of quartz using an improved single-aliquot regenerative-dose protocol. Radiat. Meas. 32, 57–73.

Murray, A.S., Wintle, A.G., 2003. The single aliquot regenerative dose protocol: potential for improvements in reliability. Radiat. Meas. 37, 377–381.

Neumann, K., Fahmy, A., Lespez, L., Ballouche, A., Huysecom, E., 2009. The Early Holocene palaeoenvironment of Ounjougou (Mali): phytoliths in a multiproxy context. Palaeogeogr. Palaeoclimatol. Palaeoecol. 276, 87–106.

Nott, J.F., Thomas, M.F., Price, D.M., 2001. Alluvial fans, landslides and Late Quaternary climatic change in the wet tropics of northeast Queensland. Aust. J. Earth Sci. 48, 875–882.

Novello, A., Barboni, D., Berti-Equille, L., Mazur, J.-C., Poilecot, P., Vignaud, P., 2012. Phytolith signal of aquatic plants and soils in Chad, Central Africa. Rev. Palaeobot. Palynol. 178, 43–58.

Olley, J.M., Murray, A., Roberts, R.G., 1996. The effects of disequilibria in the uranium and thorium decay chains on burial dose rates in fluvial sediments. Quat. Sci. Rev. 15, 751–760.

Pearl, F.B., Dickson, D.B., 2004. Geoarchaeology and prehistory of the Kipsing and Tol river watersheds in the Mukogodo Hills region of Central Kenya. Geoarchaeol. 19, 565–582.

Phillips, J.D., Lorz, C., 2008. Origins and implications of soil layering. Earth Sci. Rev. 89, 144–155.

Piperno, D.R., Pearsall, D.M., 1998. The Silica Bodies of Tropical American Grasses: Morphology, Taxonomy, and Implications for Grass Systematics and Fossil Phytolith Identification. Smithsonian Institution Press, Washington, D.C.

Porraz, G., Parkington, J.E., Rigaud, J.-P., Miller, C.M., Poggenpoel, C., Tribolo, C., Archer, W., Cartwright, C.R., Charrié-Duhaut, A., Dayet, L., Igreja, M., Mercier, N., Schmidt, P., Verna, C., Texier, P.-J., 2013. The MSA sequence of Diepkloof and the history of southern African Late Pleistocene populations. J. Archaeol. Sci. 40.

Prescott, J.R., Hutton, J.T., 1994. Cosmic ray contributions to dose rates for luminescence and ESR dating: large depths and long-term time variations. Radiat. Meas. 23, 497–500.

Ritter, J.B., Miller, J.R., Enzel, Y., Wells, S.G., 1995. Reconciling the roles of tectonism and climate in Quaternary alluvial fan evolution. Geology 23, 245–248.

Robin, V., Petit, S., Beaufort, D., Prêt, D., 2013. Mapping kaolinite and dickite in sandstone thin sections using infrared microspectroscopy. Clays Clay Miner. 61, 141–151.

Rowan, A.V., Roberts, H.M., Jones, M.A., Duller, G.A.T., Covey-Crump, S.J., Brocklehurst, S.H., 2012. Optically Stimulated Luminescence dating of glacio-fluvial sediments on the Canterbury Plains, South Island, New Zealand. Quat. Geochronol. 8, 10–22.

Runge, F., 1999. The opal phytolith inventory of soils in Central Africa —quantities, shapes, classification, and spectra. Rev. Palaeobot. Palynol. 107, 23–53.

Sahle, Y., Morgan, L.E., Braun, D.R., Atnafu, B., Hutchings, W.K., 2014. Chronological and behavioral contexts of the earliest Middle Stone Age in the Gademotta formation, main Ethiopian Rift. Quat. Int. 331, 6–19.

Salisbury, J.W., Vergo, N., 1991. Infrared (2.1-25 μm) Spectra of Minerals. John Hopkins University Press, Baltimore, Maryland.

Schick, K.D., 1987. Modeling the formation of Early Stone Age artifact concentrations. J. Hum. Evol. 16, 789–807.

Scholz, C.A., Cohen, A.S., Johnson, T.C., King, J., Talbot, M.R., Brown, E.T., 2011. Scientific drilling in the Great Rift Valley: the 2005 Lake Malawi scientific drilling project — an overview of the past 145,000 years of climate variability in southern hemisphere East Africa. Palaeogeogr. Palaeoclimatol. Palaeoecol. 303, 3–19.

Scholz, C.A., Johnson, T.C., Cohen, A.S., King, J.W., Peck, J.A., Overpeck, J.T., Talbot, M.R., Brown, E.T., Kalindekafe, L., Amoako, P.Y.O., Lyons, R.P., Shanahan, T.M., Castaneda, I.S., Heil, C.W., Forman, S.L., McHargue, L.R., Beuning, K.R., Gomez, J., Pierson, J., 2007. East African megadroughts between 135 and 75 thousand years ago and bearing on early-modern human origins. Proc. Natl. Acad. Sci. 104, 16416–16421.

Sharon, G., Zaidner, Y., Hovers, E., 2014. Opportunities, problems and future directions in the study of open-air Middle Paleolithic sites. Quat. Int. 331, 1–5.

Shea, J.J., 2011. Homo sapiens is as Homo sapiens was. Curr. Anthr. 52, 1–35.

Sisk, M.L., Shea, J.J., 2008. Intrasite spatial variation of the Omo Kibish Middle Stone Age assemblages: artifact refitting and distribution patterns. J. Hum. Evol. 55, 486–500.

Sitzia, L., Bertran, P., Boulogne, S., Brenet, M., Crassard, R., Delagnes, A., Frouin, M., Hatté, C., Jaubert, J., Khalidi, L., Messager, E., Mercier, N., Meunier, A., Peigné, S., Queffelec, A., Tribolo, C., Macchiarelli, R., 2012. The paleoenvironment and lithic taphonomy of Shi'Bat Dihya 1, a Middle Paleolithic site in Wadi Surdud, Yemen. Geoarchaeology 27, 471–491.

Stewart, B.A., Dewar, G.I., Morley, M.W., Inglis, R.H., Wheeler, M., Jacobs, Z., Roberts, R.G., 2012. Afromontane foragers of the Late Pleistocene: site formation, chronology and occupational pulsing at Melikane Rockshelter, Lesotho. Quat. Int. 270, 40–60.

Stone, J.R., Westover, K.S., Cohen, A.S., 2011. Late Pleistocene paleohydrography and diatom paleoecology of the central basin of Lake Malawi, Africa. Palaeogeogr. Palaeoclimatol. Palaeoecol. 303, 51–70.

Stoops, G., 2003. Guidelines for Analysis and Description of Soil and Regolith Thin Sections. Soil Science Society of America, Inc., Madison, Wisconsin.

Thomas, M.F., 2003. Landscape sensitivity to rapid environmental change—a Quaternary perspective with examples from tropical areas. CATENA 55, 107–124.

Thompson, J., Mackay, A., de Moor, V., Gomani-Chindebvu, E., 2014. Catchment survey in the Karonga district: a landscape-scale analysis of provisioning and core reduction strategies during the Middle Stone Age of northern Malawi. Afr. Archaeol. Rev. 31, 447–478.

Thompson, J.C., Mackay, A., Wright, D.K., Welling, M., Greaves, A., Gomani-Chindebvu, E., Simengewa, D., 2012. Renewed investigations into the Middle Stone Age of northern Malawi. Quat. Int. 270, 129–139.

Thompson, J.C., Welling, M., Gomani-Chindebvu, E., 2013. Using GIS to integrate old and new archaeological data from Stone Age deposits in Karonga, Malawi. Int. J. Herit. Digital Era 2, 611–630.

Tierney, J.E., Russell, J.M., Huang, Y., Damsté, J.S.S., Hopmans, E.C., Cohen, A.S., 2008. Northern hemisphere controls on tropical southeast African climate during the past 60,000 years. Science 322, 252–255.

Tryon, C.A., 2010. How the geological record affects our reconstructions of Early Middle Stone Age settlement patterns: the case of an alluvial fan setting for Koimilot (Kapthurin formation), Kenya. In: Conard, N.J., Delagnes, A. (Eds.), Settlement Dynamics of the Middle Paleolithic and Middle Stone Age, Volume IIIKerns Verlag, Tübingen, Germany, pp. 39–66.

Tryon, C.A., Faith, J.T., 2013. Variability in the Middle Stone Age of Eastern Africa. Curr. Anthr. 54, S234–S254.

Twiss, P.C., Suess, E., Smith, R.M., 1969. Morphological classification of grass phytoliths. Soil Sci. Soc. Am. Proc. 33, 109–115.

Van de Marel, H.W., Beutelspacher, H., 1976. Atlas of Infrared Spectroscopy of Clay Minerals and Their Admixtures. Elsevier, Amsterdam.

Van Nest, J., 2002. The good earthworm: how natural processes preserve upland Archaic archaeological sites of western Illinois, U.S.A. Geoarchaeology 17, 53–90.

Vincens, A., Chalié, F., Bonnefille, R., Tiercelin, J., 1993. Pollen-derived rainfall and temperature estimates for Lake Tanganyika and their implication for Late Pleistocene water levels. Quat. Res. 40, 343–350.

Wang, C.-y., Cheng, L.-H., Chin, C.-V., Yu, S.-B., 2001. Coseismic hydrologic response of an alluvial fan to the 1999 Chi-Chi earthquake. Taiwan. Geol. 29, 831–834.

Waters, J.V., Jones, S.J., Armstrong, H.A., 2010. Climatic controls on Late Pleistocene alluvial fans. Cyprus. Geomorphol. 115, 228–251.

White, F., 1983. The Vegetation of Africa: a Descriptive Memoir to Accompany the UNESCO/AETFAT/UNSO Vegetation Map of Africa. UNESCO, Paris.

Wright, D.K., Thompson, J., Mackay, A., Welling, M., Forman, S.L., Price, G., Zhao, J.-x., Cohen, A.S., Malijani, O., Gomani-Chindebvu, E., 2014. Renewed geo-archaeological investigations of Mwanganda's village (Elephant Butchery Site), Karonga, Malawi. Geoarchaeology 29, 98–120.

Yellen, J.E., 1996. Behavioural and taphonomic patterning at Katanda 9: a Middle Stone Age site, Kivu Province, Zaire. J. Archaeol. Sci. 6, 915–932.

Zipkin, A., Hanchar, J., Brooks, A.S., Grabowski, M.W., Thompson, J.C., Gomani-Chindebvu, E., 2015. Ochre fingerprints: distinguishing among Malawian mineral pigment sources with homogenized ochre chip LA-ICPMS. Archaeometry 57, 297–317.